

Novel Fe–Pd/ γ -Al₂O₃ catalysts for the selective hydrogenation of C≡C bonds under mild conditions

Anastasiya A. Shesterkina,^{*,a} Ludmila M. Kozlova,^a Igor V. Mishin,^a Olga P. Tkachenko,^a Gennady I. Kapustin,^a Viktor P. Zakharov,^b Mikhail S. Vlaskin,^b Andrei Z. Zhuk,^b Olga A. Kirichenko^a and Leonid M. Kustov^{a,c}

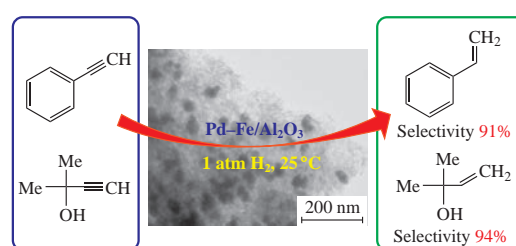
^a N. D. Zelinsky Institute of Organic Chemistry, Russian Academy of Sciences, 119991 Moscow, Russian Federation. Fax: +7 499 135 5328; e-mail: anastasiia.strelkova@mail.ru

^b Joint Institute of High Temperatures, Russian Academy of Sciences, 125412 Moscow, Russian Federation

^c Department of Chemistry, M. V. Lomonosov Moscow State University, 119991 Moscow, Russian Federation

DOI: 10.1016/j.mencom.2019.05.034

Novel promising Fe–Pd/ γ -Al₂O₃ catalysts for the selective liquid-phase hydrogenation of unsaturated compounds (phenylacetylene and 2-methylbut-3-yn-2-ol) under ambient conditions have been prepared. They were characterized by low temperature nitrogen adsorption, XRD, SEM, TEM, TPR-H₂ and DRIFTS-CO techniques. The presence of Pd–Fe nanoparticles led to increased reactivity and selectivity of the new catalysts in hydrogenation of the C≡C bond to the C=C one as compared to those of the Pd/Al₂O₃ system.



Selective hydrogenation of C≡C to C=C bonds is a key step in the synthesis of many important products in petrochemical industry as well as of fine and special chemicals (*i.e.*, vitamins A and E, linalool, *etc.*).^{1–5} Supported Pd-containing catalysts are usually applied for selective hydrogenation due to their unique ability to promote adsorption of hydrogen, relative stability in air environment, and easy recyclability.^{6–10} Drawbacks of this system include high palladium loadings, deactivation, and toxicity.^{3,10–12,14} An addition of the second metal or metal oxide to Pd-based catalysts and the use of some hybrid systems are known as increasing the activity and selectivity of catalysts.^{15–18} The well-known bimetallic compositions for selective alkyne hydrogenation include Pd–In,¹⁹ Pd–Zn,^{14,17,20,21} Pd–Ag,²² and Pd–Cu.^{23,25} However, the Fe influence on the catalytic properties of Pd catalysts in the mentioned reactions remains scarcely investigated. There is increasing research interest in iron as a catalyst component for the homogeneous and heterogeneous hydrogenation since this transition metal is abundant in nature, cheap, non-toxic, and potentially amenable to magnetic recovery.^{16,26,27} The support material plays a crucial role in the overall catalytic performance for achieving the high conversion and better selectivity towards the desired products.^{3,28} Despite the large number of reports on the selective hydrogenation on Pd-containing catalysts, the improvements in efficiency and environmental safety of catalytic systems are remaining an active area of research and development.

The present work was aimed at the synthesis of the supported bicomponent Fe–Pd/ γ -Al₂O₃ catalysts.[†] The prepared materials

[†] A carrier γ -Al₂O₃ (SBET of 240 m² g^{−1}, V_{mesopore} of 1.4 cm³ g^{−1}, $V_{\text{micropore}}$ of 0.005 cm³ g^{−1}) was obtained by a thermal decomposition of boehmite at 600 °C in air. Supported bimetallic Pd(3%)–Fe(8%) catalysts were prepared by a simultaneous incipient wetness impregnation of the γ -Al₂O₃ carrier with aqueous solutions of [Pd(NH₃)₄]Cl₂·H₂O (pure, 41.42% of Pd; Aurat, Russia) and (NH₄)₃[Fe(C₂O₄)₃]·3H₂O (pure, 98%, Acrus Organics) according to the reported procedures.^{29,30} The impregnated samples were dried at 60 °C for 12 h. Thermal treatment of dry samples was carried out under different conditions: (i) calcination

were investigated by N₂ adsorption–desorption measurements, TPR-H₂, XRD, DRIFTS-CO, SEM and TEM methods. Physico-chemical properties of this system and its catalytic activity in the selective liquid-phase hydrogenation of phenylacetylene and 2-methylbut-3-yn-2-ol (dimethylethynyl carbinol or DMEC) under mild conditions were explored, and the influence of thermal treatment of the samples on the activity and selectivity of the hydrogenation processes was elucidated. 2-Methylbut-3-en-2-ol (DMVC) obtained by selective hydrogenation of DMEC is an important starting material for the production of vitamins A and E. The selective hydrogenation of phenylacetylene into styrene is of significant industrial and scientific interest, since phenylacetylene is a poisoning impurity in styrene feedstocks, causing deactivation of styrene polymerization catalysts.

The XRD results for the support and bimetallic PdFe catalysts are given in Online Supplementary Materials. The peaks recorded for the support correspond to the main diffraction peaks of γ -Al₂O₃ [Figure S1(a)]. The calcination in an air flow with the subsequent reduction of the samples in H₂ resulted in the formation of X-ray amorphous phases [Figure S1(b),(c)]. The formation

in flowing air at 400 °C for 3 h (A), (ii) calcination in flowing N₂ at 400 °C for 3 h (N). All the calcined samples were reduced in H₂ flow at 400 °C for 3 h and then cooled to 20 °C. An organic solvent (acetone) was introduced into the reactor with the reduced sample to exclude the contact with oxygen inside the reactor and to prevent oxidation of Fe nanoparticles. The reduction temperatures were selected according to the TPR-H₂ studies. The synthesized catalysts were designated as PdFe–M–H, wherein M denotes the conditions of thermal treatment (M corresponds to the method of calcination, and H means the reduction in H₂ at 400 °C). The reduced monometallic Pd(3%)/ γ -Al₂O₃ catalysts (Pd–A–H and Pd–N–H) were prepared similarly and used as a reference.

Catalytic properties of Pd–Fe/ γ -Al₂O₃ samples were studied in a glass reactor at 20 °C in H₂ (1 atm) under vigorous shaking (600 min^{−1}) in ethanol (16 ml) (30 mg of catalysts, 0.13 M phenylacetylene or DMEC, molar ratio substrate: Pd was 290: 1) with undecane (for phenylacetylene) or isoamyl alcohol (for DMEC) as an internal standard (3 ml).

of well-crystallized Pd⁰ nanoparticles after the treatment at 400 °C in N₂ flow was readily detected [Figure S1(d)]. An average size of the primary Pd⁰ crystallites in the calcined bimetallic PdFe–N catalysts was 12–13 nm. The reduction of this sample in H₂ flow at 400 °C led to the formation of Pd⁰ nanoparticles with an average size of 15–16 nm [Figure S1(e)], however lines from any iron phases could not be detected. Taking into account the XRD data, one can conclude that the phase composition and size of primary crystallites of the supported metal depend on the calcination conditions.

The TEM images of PdFe–N catalysts (Figure S2) confirmed the formation of agglomerates of nanoparticles with an average size of 20 nm. The further reduction of this sample in H₂ flow at 400 °C led to the formation of larger agglomerates. Due to the complicated morphology of Al₂O₃ in addition to small and well-distributed nanoparticles on the support surface in the PdFe–A and PdFe–A–H samples, it was difficult to make any conclusion about the size and distribution of particles.

The reducibility of the calcined samples was estimated by the TPR method (Figure 1). The reduction of monometallic Fe₂O₃ supported on alumina proceeds in two steps: the conversion of Fe³⁺ to Fe⁰ via Fe²⁺ at high temperatures in the range of 380–720 °C.³¹ The dissociative chemisorption of H₂ on Pd facilitates the reduction of ferric species at much lower temperatures.³² This trend was observed for all the bimetallic Pd–Fe catalysts in this work. However, the TPR profiles of the calcined samples were different.

Initial adsorption of H₂ on a sample calcined in the flowing air can be observed at –10 °C. Three ranges can be recognized on the adsorption curves: from –10 to 370, 370–630 and 630–850 °C. After 850 °C, the sample was kept at *T*_{max} until the H₂ consumption became negligible. The amounts of adsorbed H₂ in these three regions were 0.813, 0.108 and 0.189 mmol g^{–1}, respectively. The first area is related to the reduction of PdO. The total amount of Pd in the sample was 0.282 mmol g^{–1}. However, the H₂ amount corresponding to the first adsorption peak (maximum at 60 °C) is almost 3 (2.88) times higher than needed for the PdO reduction. Therefore, it can be suggested that the reduction of Fe₂O₃ begins at the temperature as low as ~100 °C. In this region, a shoulder is observed on the hydrogen adsorption curve. The total amount of Fe was 1.432 mmol g^{–1}, thus for the reduction of Fe³⁺ to Fe⁰, 2.149 mmol g^{–1} of H₂ was required. The total amount of H₂ needed for the reduction of both iron and palladium cations to metals was 2.431 mmol g^{–1}. At the same time, 0.998 mmol g^{–1} of H₂ was sufficient for processes: Fe³⁺ → Fe²⁺ and Pd²⁺ → Pd⁰.

For the sample calcined in the flowing air, the total amount of adsorbed H₂ was 1.11 mmol g^{–1}. This allowed us to conclude that Fe₂O₃ was reduced to FeO under the applied conditions (from –100 to 850 °C, 5% H₂/Ar, 30 ml min^{–1}, and heating rate of 10 °C min^{–1}).

In the case of sample calcined in the flowing N₂, a decrease in the absorption of hydrogen in the region of 0–370 °C was observed, whereas the spectra were practically coincided at the

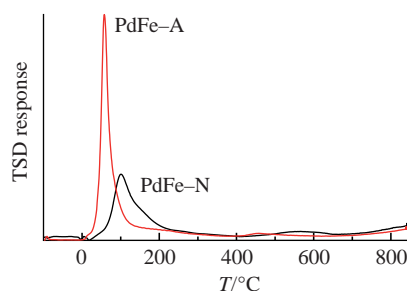


Figure 1 TPR-H₂ profiles of Pd–Fe/Al₂O₃ samples. All data are normalized to 1 g sample.

temperature above 200 °C. The absorption of H₂ at low temperatures was decreased nearly twofold. It seems that the decomposition of ammonia complexes of precursors leads to the reduction of Pd²⁺. The total calculated uptake of H₂ until 850 °C was 0.840 mmol g^{–1}, *i.e.*, almost all the hydrogen was consumed by the reduction of iron, while about half of the palladium was deoxidized by ammonia. This was confirmed by the XRD and DRIFTS data.

The acquired data indicate that the iron reduction in the presence of metallic Pd is already started at room temperature. Most likely, once metallic Pd was produced, the Fe reduction begins.

Metals states in catalysts Fe–Pd/Al₂O₃ were spectroscopically estimated using DRIFTS-CO (Figure 2). Several bands are visible in the spectrum of calcined catalyst PdFe–N [see Figure 2(a)]. The band at 2168 cm^{–1} characterizes linear carbonyl group at divalent iron cations (Fe²⁺–CO). Upon increasing the CO desorption temperature, the position of Fe²⁺–CO carbonyl band does not change, but the intensity gradually decreases (Figure S3). After desorption of CO at room temperature, the band at 2107 cm^{–1} was resolved into two bands at 2128 and 2088 cm^{–1}, belonging to linear carbonyls at monovalent palladium cations (Pd⁺–CO) and on metallic palladium (Pd⁰–CO), respectively. The bands in the region of 1992–1933 cm^{–1} correspond to bridged carbonyls on monovalent palladium cations (Pd⁺–CO–Pd⁺) and metal palladium (Pd⁰–CO–Pd⁰) (Figure S3). When CO was desorbed *in vacuo* at 200 °C, the bands from iron and palladium carbonyls disappear completely in the spectrum. The absence of any shift of the band of palladium carbonyls during thermal desorption (20–100 °C) and the sufficiently high intensity of the bridged adsorption bands indicate a low degree of dispersion of the palladium crystallites.

DRIFT-CO spectra of the reduced PdFe–N–H catalyst contains four bands at 2162, 2081, 2034 and 1958 cm^{–1} [see Figure 2(a)]. The strong band at 2162 cm^{–1} characterizes linear carbonyls on divalent iron cations (Fe²⁺–CO). The low ones at 2081 and 2034 cm^{–1} correspond to linear carbonyls on two metal centers

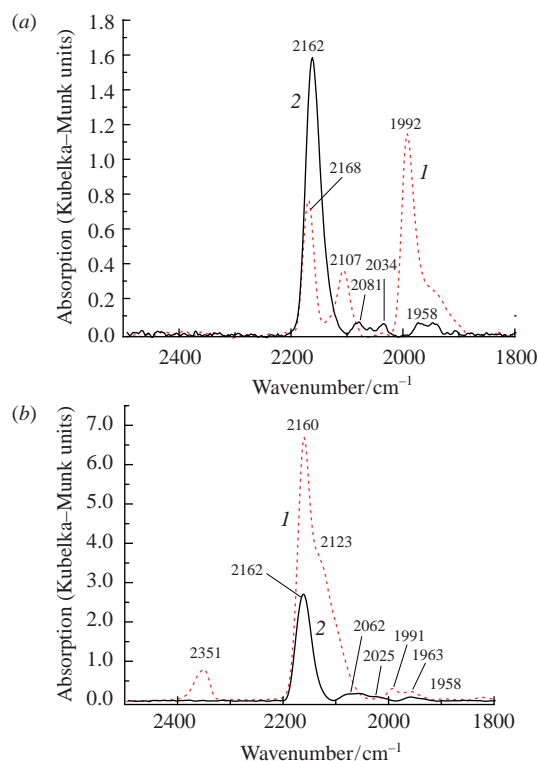


Figure 2 DRIFT-CO spectra of (1) calcined and (2) subsequently reduced (a) PdFe–N and (b) PdFe–A catalysts.

of palladium possessing different local environments, and the bands near 1958 cm^{-1} are assigned to the bridged carbonyls on metallic palladium ($\text{Pd}^0\text{-CO-Pd}^0$). In addition, all the bands disappeared from the spectrum upon evacuation of the sample at 20°C (Figure S4, see Online Supplementary Materials).

In contrast to the DRIFT-CO spectra of the PdFe–N catalyst, those of sample PdFe–A calcined in an air flow exhibited a band at 2351 cm^{-1} , which can be assigned to adsorbed CO_2 formed *via* the reduction of Fe^{3+} cations by carbon monoxide, along with an intense band at 2160 cm^{-1} attributed to linear carbonyl on divalent iron cations ($\text{Fe}^{2+}\text{-CO}$) [see Figure 2(b)]. The appearance of the bands for linear carbonyls at 2123 cm^{-1} ($\text{Pd}^+\text{-CO}$) and 2103 cm^{-1} ($\text{Pd}^0\text{-CO}$), as well as for bridged carbonyls on monovalent cations of palladium ($\text{Pd}^+\text{-CO-Pd}^+$) and metal centers of palladium ($\text{Pd}^0\text{-CO-Pd}^0$) in the region of $1991\text{--}1960\text{ cm}^{-1}$ were observed in the spectra. During CO desorption *in vacuo* at $20\text{--}100^\circ\text{C}$, the position of the $\text{Fe}^{2+}\text{-CO}$ carbonyl bands did not change, while their intensity was gradually decreased (Figure S5). The absence of any shift of the band from the carbonyls of palladium during thermal desorption along with a sufficiently high intensity of the bands from the bridged adsorption forms at the palladium centers indicate a low dispersion of the palladium metal particles. It is consistent with the XRD results for this sample [see Figure S1(d)]. In the spectrum of CO adsorbed on the surface of the reduced catalyst PdFe–A–H, the band at 2351 cm^{-1} was not detected, thus, all the palladium was in the metallic state. The bands at 2062 and 2025 cm^{-1} belong to linear carbonyls at two metal centers of palladium possessing different local environments, and the 1958 cm^{-1} band is attributed to bridged carbonyls on metallic palladium. In addition, all the bands disappeared during the evacuation of the sample at 20°C (Figure S6).

The summarized results of the DRIFT-CO experiments for the calcined catalysts are given in Online Supplementary Materials (Figure S7). Thus, the comparison of the DRIFT-CO spectra of the Pd–Fe/ Al_2O_3 catalysts prepared under various conditions suggests the formation of different bimetallic phase in the samples.

Catalytic activity of the prepared Pd and Pd–Fe samples in liquid-phase hydrogenation of unsaturated compounds (phenylacetylene and 2-methylbut-3-yn-2-ol) under ambient conditions is summarized in Table 1. The monometallic iron samples (both calcined and reduced in a H_2 flow at 400°C) were catalytically inactive under the reaction conditions. The activities of synthesized monometallic catalysts Pd–A–H and Pd–N–H were 15 and 25 times higher than that of the Lindlar catalyst (5% Pd/ CaCO_3 inhibited by the lead complexes) in the reaction of phenylacetylene hydrogenation, respectively. However, the selectivity towards styrene was lower than that of the Lindlar catalyst (see Table 1, entry 2), while the Pd–N–H sample was more active than the monometallic sample calcined in an air flow. The modification of monometallic palladium samples with iron has significantly changed their catalytic properties. Catalytic performance of bimetallic Pd–Fe/ Al_2O_3 catalysts in the hydrogenation of phenylacetylene depends primarily on the calcination procedure and hence on the nature of active sites and the particle size. Comparing the calcined Pd–Fe/ Al_2O_3 samples, one may conclude that at a similar initial rate of hydrogenation, the maximum selectivity to styrene (87%) at the complete conversion of phenylacetylene was observed in the case of PdFe–N sample (see Table 1, entry 6). According to the XRD, TEM and TPR- H_2 analyses, calcination in a N_2 flow at 400°C led to the formation of well-crystallized Pd^0 nanoparticles with the size of 15 nm, whereas the sample calcined in air (PdFe–A) was X-ray amorphous and consisted mainly of the Pd^0 and Fe^{3+} and Fe^{2+} oxides. A further reduction of all the calcined samples in an H_2 flow at 400°C increased their selectivity to styrene and activity. However, the highest selectivity

Table 1 Catalytic properties of the 3Pd–8Fe/ Al_2O_3 catalysts in selective hydrogenation of the $\text{C}\equiv\text{C}$ bonds.^a

Entry	Catalyst	Substrate	Product	t^b/min	$S_{\text{substrate}}^{99}$ (%)	$r_0^c/\text{mol}_{\text{substrate}}/\text{mol}_{\text{Pd}}\text{ s}^{-1}$
1	Lindlar	Phenylacetylene	Styrene	150	87	0.05
2	Pd–A–H			10	79	0.39
3	PdFe–A			11	72	0.51
4	PdFe–A–H			5.5	85	1.19
5	Pd–N–H			4.6	75	0.99
6	PdFe–N			11	87	0.45
7	PdFe–N–H			8	91	0.59
8	Lindlar	DMEC	DMVC	32	89	0.09
9	Pd–N–H			6	80	0.87
10	PdFe–N–H			9.5	94	0.78

^aReaction conditions: $C_{\text{substrate}} = 0.13\text{ mol dm}^{-3}$, $m_{\text{catalyst}} = 0.03\text{ g}$, H_2 (1 atm), room temperature, $n_{\text{substrate}}:n_{\text{Pd}} = 290:1$. ^bTime required for the complete conversion of the substrate. ^cInitial hydrogenation rate calculated at the conversion of the substrate not exceeding 10%.

(91%) was observed for the sample PdFe–N–H (see Table 1, entry 7).

The catalytic properties of the sample PdFe–N–H were studied in the hydrogenation of the $\text{C}\equiv\text{C}$ bond in an unsaturated alcohol. The selectivity towards DMVC on this catalyst under mild reaction conditions was 95% at the complete DMEC conversion at a high rate of hydrogenation (see Table 1, entry 10).

The reduced Pd–Fe/ Al_2O_3 samples demonstrated promising magnetic properties and were easily separated from the reaction solution with a permanent magnet (Figure 3). The catalytic activity and the selectivity remained high even after four successive catalytic recycles (Figure 4). In addition, no metal leaching occurred during the cyclic operation after four cycles.

In conclusion, the novel Pd–Fe/ Al_2O_3 catalysts for the selective hydrogenation of alkynes into alkenes were prepared. The catalytic properties of the bimetallic catalysts depend on the conditions of thermal treatment of their precursors. The calcination process has significantly affected the palladium dispersion. The presence of Fe in Pd–Fe/ Al_2O_3 catalyst modifies the catalytic behavior of Pd. The formation of Pd–Fe bimetallic phase in the samples promotes their reactivity and selectivity. The best results on the selective styrene formation (91% at the 100% conversion of phenylacetylene) and DMVC (95% at the 100% conversion of DMEC) were observed for the sample calcined in N_2 flow at 400°C and

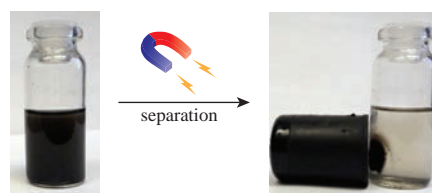


Figure 3 The magnetic separation of the reduced PdFe–N–H catalyst from the reaction solution.

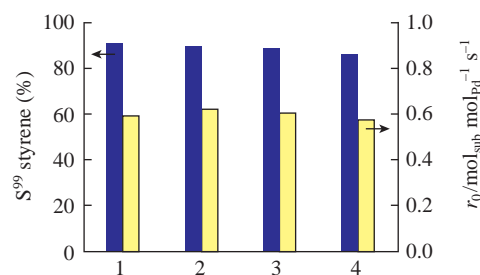


Figure 4 Reusability of the PdFe–N–H catalyst in four consecutive cycles of phenylacetylene hydrogenation.

then reduced in H₂ flow at 400 °C. Thus, our stable magnetic Pd–Fe/Al₂O₃ catalysts are a good alternative to the traditional toxic Lindlar catalyst in the selective alkyne hydrogenation under mild conditions.

Electron microscopy characterization was performed at the Department of Structural Studies of N. D. Zelinsky Institute of Organic Chemistry of the Russian Academy of Sciences. A. Shesterkina is grateful to Haldor Topsøe A/S for the financial support in the framework of PhD student support programme. The authors are grateful to E. Shuvalova for the assistance in conducting the experiments.

Online Supplementary Materials

Supplementary data associated with this article can be found in the online version at doi: 10.1016/j.mencom.2019.05.034.

References

- M. Zhang, Y. Yang, C. Li, Q. Liu, C. T. Williams and C. Liang, *Catal. Sci. Technol.*, 2014, **4**, 329.
- M. Crespo-Quesada, F. Cárdenas-Lizana, A.-L. Dessimoz and L. Kiwi-Minsker, *ACS Catal.*, 2012, **2**, 1773.
- F. P. da Silva and L. M. Rossi, *Tetrahedron*, 2014, **70**, 3314.
- E. A. Karakhanov, I. A. Aksenov, S. V. Kardashev, A. L. Maksimov, F. N. Putilin, A. N. Shatokhin and S. V. Savilov, *Appl. Catal., A*, 2013, **464–465**, 253.
- N. Semagina, A. Renken, D. Laub and L. Kiwi-Minsker, *J. Catal.*, 2007, **246**, 308.
- E. A. Karakhanov, A. L. Maximov, E. M. Zakharyan, A. V. Zolotukhina and A. O. Ivanov, *Mol. Catal.*, 2017, **440**, 107.
- E. V. Belyaeva, V. I. Isaeva, E. E. Said-Galiev, O. P. Tkachenko, S. V. Savilov, A. V. Egorov, L. M. Kozlova, V. Z. Sharf and L. M. Kustov, *Russ. Chem. Bull., Int. Ed.*, 2014, **63**, 396 (*Izv. Akad. Nauk, Ser. Khim.*, 2014, 396).
- S. Domínguez-Domínguez, Á. Berenguer-Murcia, B. K. Pradhan, Á. Linares-Solano and D. Cazorla-Amorós, *Phys. Chem.*, 2008, **112**, 3827.
- W. Yu, H. Hou, Z. Xin, S. Niu, Y. Xie, X. Ji and L. Shao, *RSC Adv.*, 2017, **7**, 15309.
- W. Zhang, F. Wang, X. Li, Y. Liu and J. Ma, *Appl. Surf. Sci.*, 2017, **404**, 398.
- H. Lindlar and R. Dubuis, *Org. Synth.*, 1966, **46**, 89.
- S. A. Nikolaev, N. A. Permyakov, V. V. Smirnov, A. Yu. Vasil'kov and S. N. Lanin, *Kinet. Catal.*, 2010, **51**, 288 (*Kinet. Katal.*, 2010, **51**, 305).
- M. Costa, P. Pelagatti, C. Pelizzi and D. Rogolino, *J. Mol. Catal. A: Chem.*, 2002, **178**, 21.
- I. S. Mashkovsky, P. V. Markov, G. O. Bragina, A. V. Rassolov, G. N. Baeva and A. Yu. Stakheev, *Kinet. Catal.*, 2017, **58**, 480 (*Kinet. Katal.*, 2017, **58**, 508).
- V. P. Ananikov, K. I. Galkin, M. P. Egorov, A. M. Sakharov, S. G. Zlotin, E. A. Redina, V. I. Isaeva, L. M. Kustov, M. L. Gening and N. E. Nifantiev, *Mendeleev Commun.*, 2016, **26**, 365.
- V. P. Ananikov, D. B. Eremin, S. A. Yakukhnov, A. D. Dilman, V. V. Levin, M. P. Egorov, S. S. Karlov, L. M. Kustov, A. L. Tarasov, A. A. Greish, A. A. Shesterkina, A. M. Sakharov, Z. N. Nysenko, A. B. Sheremetev, A. Yu. Stakheev, I. S. Mashkovsky, A. Yu. Sukhorukov, S. L. Ioffe, A. O. Terent'ev, V. A. Vil', Yu. V. Tomilov, R. A. Novikov, S. G. Zlotin, A. S. Kucherenko, N. E. Ustyuzhanina, V. B. Krylov, Yu. E. Tsvetkov, M. L. Gening and N. E. Nifantiev, *Mendeleev Commun.*, 2017, **27**, 425.
- Z. Wang, L. Yang, R. Zhang, L. Li, Z. Cheng and Z. Zhou, *Catal. Today*, 2016, **264**, 37.
- E. A. Redina, O. A. Kirichenko, A. A. Greish, A. V. Kuchero, O. P. Tkachenko, G. I. Kapustin, I. V. Mishin and L. M. Kustov, *Catal. Today*, 2015, **246**, 216.
- I. S. Mashkovsky, N. S. Smirnova, P. V. Markov, G. N. Baeva, G. O. Bragina, A. V. Bukhtiyarov, I. P. Prosvirin and A. Yu. Stakheev, *Mendeleev Commun.*, 2018, **28**, 603.
- M. Crespo-Quesada, M. Grasmann, N. Semagina, A. Renken and L. Kiwi-Minsker, *Catal. Today*, 2009, **147**, 247.
- I. S. Mashkovsky, P. V. Markov, G. O. Bragina, G. N. Baeva, A. V. Rassolov, A. V. Bukhtiyarov, I. P. Prosvirin, V. I. Bukhtiyarov and A. Yu. Stakheev, *Mendeleev Commun.*, 2018, **28**, 152.
- A. V. Rassolov, P. V. Markov, G. O. Bragina, G. N. Baeva, I. S. Mashkovskii, I. A. Yakushev, M. N. Vargafik and A. Yu. Stakheev, *Kinet. Catal.*, 2016, **57**, 853 (*Kinet. Katal.*, 2016, **57**, 857).
- P. V. Markov, G. O. Bragina, A. V. Rassolov, G. N. Baeva, I. S. Mashkovsky, V. Yu. Murzin, Ya. V. Zubavichus and A. Yu. Stakheev, *Mendeleev Commun.*, 2016, **26**, 502.
- A. J. McCue, C. J. McRitchie, A. M. Shepherd and J. A. Anderson, *J. Catal.*, 2014, **319**, 127.
- K. C. K. Swamy, A. S. Reddy, K. Sandeep and A. Kalyani, *Tetrahedron Lett.*, 2018, **59**, 419.
- V. Kelsen, B. Wendt, S. Werkmeister, K. Junge, M. Beller and B. Chaudret, *Chem. Commun.*, 2013, **49**, 3416.
- A. V. B. Reddy, Z. Yusop, J. Jaafar, Y. V. M. Reddy, A. B. Aris, Z. A. Majid, J. Talib and G. Madhavi, *J. Environ. Chem. Eng.*, 2016, **4**, 3537.
- E. A. Karakhanov, A. L. Maksimov, E. M. Zakharian, Y. S. Kardasheva, S. V. Savilov, N. I. Truhmanova, A. O. Ivanov and V. A. Vinokurov, *J. Mol. Catal. A: Chem.*, 2015, **397**, 1.
- O. A. Kirichenko, G. I. Kapustin, V. Nissenbaum, I. V. Mishin and L. Kustov, *J. Therm. Anal. Calorim.*, 2014, **118**, 749.
- L. M. Kustov, S. R. Al-Abed, J. Virkutyte, O. A. Kirichenko, E. V. Shuvalova, G. I. Kapustin, I. V. Mishin, V. D. Nissenbaum, O. P. Tkachenko and E. D. Finashina, *Pure Appl. Chem.*, 2014, **86**, 1141.
- N. Lingaiah, N. S. Babu, R. Gopinath, P. S. S. Reddy and P. S. S. Prasad, *Catal. Surv. Asia*, 2006, **10**, 29.
- F. J. Berry, X. Changhai and S. Jobson, *J. Chem. Soc., Faraday Trans.*, 1990, **86**, 165.

Received: 3rd October 2018; Com. 18/5709